The AMS Experiment on the International Space Station

Maura Graziani and Nicola Tomassetti

1 Introduction

On the 16th of May 2011, NASA's Space Shuttle *Endeavour* was launched from Cape Canaveral at the Kennedy Space Center (Florida, USA) for its last mission. The main purpose of the mission was the delivery of one of the most complex instruments ever built: the Alpha Magnetic Spectrometer (AMS), a multipurpose detector of high-energy particles designed to operate in space for a long-duration mission of fundamental physics research. A few hours after the launch, a first power-on of AMS inside the shuttle was performed remotely, with a preliminary monitoring on ground of various temperatures and electrical currents. On May 19th, AMS was powered on for installation on the International Space Station. At 4:46 a.m. the same day the installation was completed and the first activation of the full experiment in space took place. Since then, AMS is sending us a continuous flow of scientific data, adding new knowledge on a variety of fundamental physics questions. The main AMS scientific goals include the indirect search of dark matter, the search of primordial antimatter, and the understanding of fundamental astrophysical processes of cosmic rays in the Galaxy. Cosmic rays are charged particles with galactic and extra-galactic origin, coming from outer space to the Earth's atmosphere with a broad range of energy that extends over several decades. Their origin, their transport in the Galaxy, and their interactions with the matter are not yet well known, so they are subject of extensive research. Cosmic particles are mainly composed by protons ($\sim$90%), helium ($\sim$8%), heavier nuclei ($\sim$1%), electrons ($\sim$1%) and antiparticles ($<$1%). Part of them such as electrons, protons, ^{4}He, C-N-O, or Fe are believed to be of primary origin, i.e., accelerated by explosions of supernova remnants or stellar

M. Graziani (✉) · N. Tomassetti
Department of Physics and Geology, University of Perugia, 06123 Perugia, Italy
e-mail: maura.graziani@unipg.it

N. Tomassetti
e-mail: nicola.tomassetti@unipg.it

M. Streit-Bianchi et al. (eds.), *Advances in Cosmology*,
https://doi.org/10.1007/978-3-031-05625-3_12

winds, although the exact mechanisms are not yet well known [1]. Rarer CR elements such as ^{2}H, ^{3}He, Li-Be-B elements or antiparticles are believed to be of secondary origin, i.e. produced by collisions of primary nuclei with the interstellar medium. Measuring these components is crucial to understand the fundamental processes of CR acceleration and transport in the Galaxy. Moreover, the knowledge of the energy spectra of CR nuclei enables us to predict the level of secondary antimatter production in CR, which constitutes the astrophysical background for the search of dark matter induced signals. The energy spectra of CR antiparticles, such as antiprotons and positrons, are in fact recognized to be powerful observables for the search of dark matter signatures.

2 The AMS Experiment

AMS is a detector of high-energy charged particles operating onboard the International Space Station since May 2011 to conduct a long term observation of cosmic rays in near earth orbit. AMS has been conceived to address open questions in fundamental physics and astrophysics by means of accurate measurements of CR. The apparent absence of anti-matter in the Universe is still a mystery which questions the foundations of elementary particle physics and our current understanding of the origin and evolution of the cosmos. The detection of even a single anti-nucleus in the cosmic radiation, such a nucleus of $\bar{H}e$ or $\bar{C}$, could be a direct proof of the existence of antimatter domains, since the probability of their generation via spallation processes in the interstellar medium is very low [2] due to their high mass. Searches for nuclear anti-matter has been carried by now since more than 30 years with increasing sensitivity in continuously extending energy ranges, with no positive detection [3]. The large amount of CR particles that AMS will be able to collect during its mission (as of today more than 190 billion particles) will allow to search for anti-nuclei with unprecedented sensitivity.

Another primary discovery potential for AMS concerns the indirect dark matter detection. Dark matter could be detected in CR through its annihilation into standard particles and γ resulting in deviations or structures to be seen in the cosmic ray spectra. Due to the low intensity of fluxes coming from DM annihilation, detection of an excess can be possible only in the rarest CR components, i.e. anti-protons, positrons or anti-deuteron (never observed so far) which are not routinely produced at astrophysical sources.

A further objective of AMS, is the accurate measurements of all the charged species of the CR, including chemical species up to Iron and isotopes up to Carbon. These measurements are needed to address open questions in the origin and propagation of CR in our galaxy.

With a size of $2\times3\times4$ m^3 size for an overall weight of 7.5 tons and a total power consumption <2 kW, AMS takes full advantage of the state of-the art detector technology developed for high energy experiments operating at particle accelerators. I The instrument will be active for the entire ISS lifetime, i.e., until 2028 or beyond.

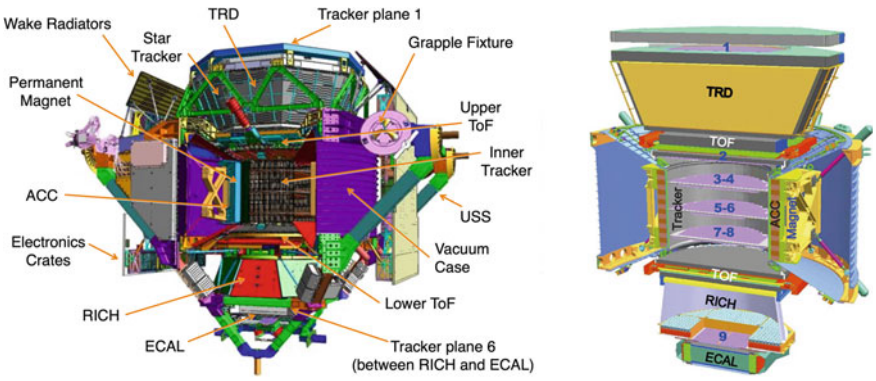

Fig. 1 Two schematic views of AMS. The various detectors are labelled

With this long observation time and its large acceptance ($\sim$0.5 m^2sr), AMS can provide high-quality data on CR fluxes at the TeV energy scale with unprecedented precision and sensitivity. Furthermore, the measurements of low energy CR fluxes over an entire 11-year solar cycle will enable us to perform a multichannel investigation of the solar modulation effect of Galactic CR.

2.1 The Detector

To fulfill its ambitious scientific objectives, AMS has been conceived as a particle physics experiment, with a high degree of redundancy in measuring the characteristics of the incident particles, satisfying at the same time the stringent requirements in reliability that are needed to survive to the hostile environment in space. Figure 1 shows a schematic view of the detector: the core of the instrument is the magnetic spectrometer composed of a permanent magnet, which produces a magnetic field with an intensity of 0.15 T, and of 9 layers of double-sided silicon micro-strip sensors that constitute the Tracker.

The task of the spectrometer is the measurement of particle rigidity ($R = P/eZ$, momentum/charge ratio) by mean of the reconstruction of the particle trajectory along the Tracker layers with $\sim 10\,\mu$m ($\sim 30\,\mu$m) of spatial resolution on the Y (X) side. Above and below the spectrometer two planes of time of flight counters (ToF) provide the main trigger of AMS and distinguish between up-going and down-going particles. This information, combined with the trajectory curvature given by the spectrometer, is used to reconstruct the sign of the charge. The spectrometer and the ToF constitute the key instruments for matter-antimatter separation. A Transition Radiation Detector (TRD) is located at the top of the instrument. The detector ends with a Ring Imaging Cherenkov detector (RICH) and an electromagnetic calorimeter (ECAL). The central part of AMS is surrounded by an anti-coincidence system (ACC)

that provides the veto signal in the trigger for the particles detected outside the field of view of the instrument.

The particle absolute charge (Z) is measured independently by each Tracker layers, by the ToF and the RICH. This redundancy allows to evaluate the fragmentation of high Z nuclei along the detector. The velocity $\beta = v/c$ can be determined from the transit time between the ToF planes (for Z = 1, $\Delta\beta/beta \sim 3\%$), or more precisely using the RICH system (for Z = 1, $\Delta\beta/beta \sim 0.1\%$).

In the measurement of CR leptons, the signals in TRD and ECAL are used to discriminate the leptonic component from the hadronic background. The combination of these information allows for an efficient lepton/hadron separation power. AMS instrument is described in details in Sect. 3.

3 AMS Results over 10 Years of Data Taking

In the following the main results obtained by AMS over 10 years of data taking will be discussed. The results include the fluxes of positrons, electrons, antiprotons, protons, and nuclei. The isotropic flux for a given specie x of CR, Φ_i, in the ith bin of energy ΔE_i, or in the ith bin of rigidity ΔR_i is given by:

$$\Phi_i = \frac{N_i}{A(1+\delta_i)T_i \Delta E_i (\Delta R_i)} \tag{1}$$

where:

- N_i is the number of events tagged as x in bin i corrected for the bin to-bin migration using the unfolding procedure described in [4].
- A_i is the corresponding effective acceptance that includes geometric acceptance, and the trigger and selection efficiencies, and is calculated from Monte Carlo simulation.
- T_i is the data collection time.
- δ_i is the data/MonteCarlo correction to the Acceptance, estimated by comparing the efficiencies in data and Monte Carlo simulation of every selection cut using information from the detectors unrelated to that cut.

3.1 Results on CR Leptons

Electrons (e^-) and positrons (e^+) constitute respectively the $\sim 1 - 0.1\%$ and $\sim 0.1 - 0.01\%$ (depending on energy) of the total CR radiation. The observed e^- are mainly Primaries, i.e. directly produced from the CR sources, while e^+ are secondaries, i.e. produced by the collisions of CR with the interstellar medium. Even if they constitute a rare component of CR, $e^{\pm}$ carry important physics information. Due to their low

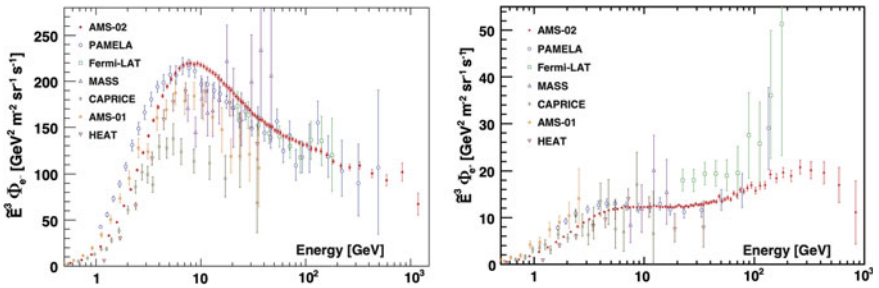

Fig. 2 The AMS electron (on the left) and positron (on the right) spectrum multiply by E^3 together with earlier measurements from PAMELA [5], Fermi-LAT [6], MASS [7], CAPRICE [8], AMS-01 [9], and HEAT [10, 11]

mass, are subject to important energy losses due to interaction with the interstellar medium, in their trajectory between the sources and Earth, representing a unique probes to study the CR sources property in the galactic neighborhood and a gold channel for the indirect search of dark matter.

The first publication on this subject from PAMELA, in early 2009, clearly showed a steady increase of the positron fraction [5] and this opened the road to a world-wide effort to account for new e^+ sources contributing to the flux. Measurements from Fermi were confirming the trend shown by PAMELA, even if the dispersion of the FERMI data with respect to the PAMELA and the following AMS measurements clearly shows the limits of the indirect charge measurement technique. The real breakthrough in these measurements came however with AMS results ams, ams2, ams3, ams4, ams5. Thanks to the large acceptance and the high electron/proton discriminating power, obtained combining the independent information coming from TRD and ECAL, AMS has provided precise measurements in an extended energy range.

Figure 2 shows the AMS electron (on the left) and positron (on the right) spectrum multiply by E^3 together with earlier experiments [5–10]. The electron flux has been measured in the energy range from 0.5 GeV to 1.4 TeV based on 28.1×10^6 electrons. The positron flux has been measured in the energy range from 0.5 GeV to 1 TeV and is based on 1.9 million of positrons. The AMS data significantly extend the measurements into the uncharted high-energy region. The behavior of the electron and positron as a function of energy is distinctly different.

The rise observed in the e^+ flux starting from 25.2±8 GeV, compared with the lower-energy trend, can be explained only taken into account an extra source of e^+ respect to the secondary production in the interstellar medium. As shown in Fig. 3 (left) in the entire energy range the e^+ flux is well described by the sum of two terms: "diffuse" term associated with the secondary positrons from cosmic ray collisions and the source term which has an exponential energy cutoff of 810^{+310}_{-180} GeV (see [12] for more details).

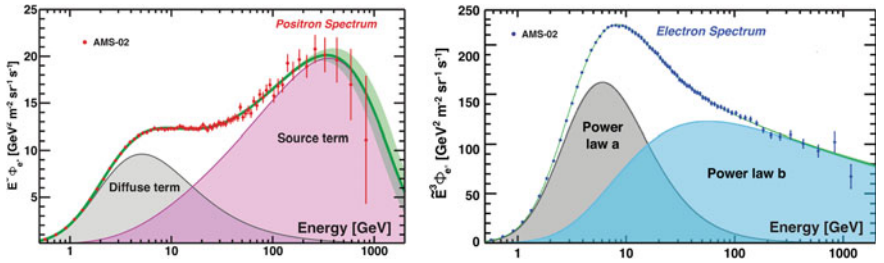

Fig. 3 On the left: The red data points represent the measured positron flux multiply by E^3. The source term contribution is represented by the magenta area and the diffuse term contribution by the gray area. On the right: the blue data points represent the measured electron flux multiply by E^3. The two power law components a and b are represented by the gray and blue areas, respectively

The source term can originate either from dark matter annihilation or from other astrophysical sources and the current AMS data are consistent whit both hypothesis [13–17]. More statistics at high energy is needed in order to assess the nature of the the source.

As shown in Fig. 3 (right) the electron flux is well described by the sum of two power law components. The flux exhibits a significant excess starting from $42.1^{+5.4}_{-5.2}$ GeV compared to the lower energy trends, but the nature of this excess is different from the positron flux excess above 25.2±8 GeV. Contrary to the positron flux, which has an exponential energy cutoff of 810^{+310}_{-180} GeV, at the 5σ level the electron flux does not have an energy cutoff below 1.9 TeV. The different behavior of the CR electrons and positrons measured by AMS is a clear evidence that most high energy electrons originate from different sources than high energy positrons.

An hint on the the nature of the source can be address from the measurement of anisotropies of electron and positron fluxes. Astrophysical point sources like pulsars will imprint a higher anisotropy on the arrival directions of energetic positrons [18, 19] than a smooth dark matter halo. If the excess of positrons has a dark matter origin, it should be isotropic. Both electron and positron fluxes are found to be consistent with isotropy with an upper limit on the amplitude of the dipole anisotropy for any axis in galactic coordinates of $\delta < 0.019$ (for positrons) and $\delta < 0.005$ for electrons at the 95% confident level [20].

3.2 Results on CR Nuclei

The first results on cosmic nuclei from AMS came in 2015 with the publication of the light nuclei flux of Hydrogen (protons) and Helium [4, 22]. The AMS data show that both species are described by a broken power-law in rigidity, as the fluxes experience a progressive spectral hardening at about 350 GV of rigidity. These results confirm the early findings of the ATIC-2, CREAM and PAMELA experiments [23].

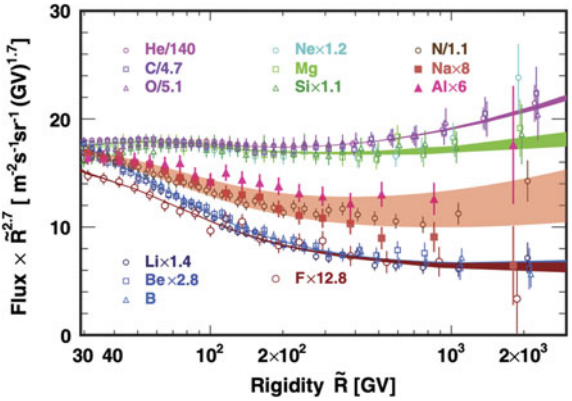

Fig. 4 The fluxes of cosmic nuclei measured by AMS as a function of rigidity from Z = 2 to Z = 14 above 30 GV. As seen, there are two classes of primary cosmic rays, He-C-O and Ne-Mg-Si, and two classes of secondary cosmic rays, Li-Be-B and F. Nitrogen (N), sodium (Na), and aluminum (Al), belong to a distinct group and are the combinations of primary and secondary cosmic rays. For clarity, data points above 400 GV are displaced horizontally. For display purposes only, fluxes were rescaled as indicated. The shaded tan band on N, Na, and Al is to guide the eye

Also, the proton-to-helium ratio at $R > 45$ GV if found to falls off steadily as p/He $R^{-0.077}$. Interpretations for these phenomena fall into three classes: diffusive shock acceleration mechanisms, propagation effects, or superposition of local and distant sources [24–27]. The origin of the CR spectral hardening (and its connection with the p/He ratio anomaly [28, 29]) is a open question that may be resolved with high-energy data on light CR nuclei. As of today, AMS has provide the measurement of:

- CR primary nuclei fluxes of Proton, Helium, Carbon, Oxygen , Neon, Magnesium and Silicon;
- CR secondary nuclei of antiproton, Litio, Beryllium, Boron and Fluorine;
- CR nuclei fluxes of Sodium, Nitrogen and Aluminium that are a combination of primary and secondary

Primary cosmic rays are thought to be mainly produced and accelerated in astrophysical sources. The precise knowledge of their spectra in the GV—TV rigidity range provides important information on the origin, acceleration, and propagation processes of cosmic rays in the Galaxy.

The AMS results shows that both primary and secondary nuclei fluxes deviate from a single power law above 200 GV, however, the rigidity dependence are distinctly different as shown in Fig. 4 that presents cosmic nuclei fluxes measured by AMS as a function of rigidity from Z = 2 to Z = 14. There are two classes of primary cosmic rays, He-C-O and Ne-Mg-Si, and two classes of secondary cosmic rays, Li-Be-B and F [30]. N, Na, and Al belong to a distinct group and are the combinations of primary and secondary cosmic rays. These results indicate there are two kinds of cosmic ray rigidity dependencies. These observations have generated new developments in

cosmic ray models [31, 32]. The theoretical models have their limitations, as none of them predicted the observed spectral behavior of the cosmic rays. The results on heavier primary cosmic rays Ne, Mg, and Si show that primary cosmic rays have at least two distinct classes of rigidity dependence. These unexpected results together with ongoing measurements of heavier elements in cosmic rays will enable us to determine how many classes of rigidity dependence exist in both primary and secondary cosmic rays and provide important information for the development of the theoretical models.

To examine the difference between the rigidity dependence of primary and secondary cosmic rays in detail, the ratios of the lithium, beryllium, and boron fluxes to the carbon and oxygen fluxes were computed. Precise knowledge of the charge and rigidity dependence of the secondary cosmic ray fluxes and the secondary to primary flux ratios is essential in the understanding of cosmic ray propagation. In particular B/C or the more direct B/O, have been traditionally used to study the propagation of cosmic rays in the Galaxy [32]. For the first time, AMS has provided the first measurement of He isotopes fluxes. This measurement can provide complementary information to the commonly used B/C or C/O ratio [33]. Helium nuclei are the second most abundant cosmic ray. They consist of two isotopes, ^{3}He and ^{4}He. ^{4}He are thought to be mainly produced and accelerated in astrophysical sources, while ^{3}He are overwhelmingly produced by the collisions of ^{4}He with the interstellar medium.

Helium interaction cross sections with the interstellar medium are significantly smaller than that of heavier nuclei. Therefore, helium travel larger distances, probing a larger galactic volume. Explicitly, the ratio ^{3}He/^{4}He probes the properties of diffusion at larger distances [34].

Protons and their anti-particle (anti-protons) can contribute to the indirect search of Dark Matter. The antiprotons constitute, as in the case of positrons, a rare component of CR: for each antiproton there are approximately 10^4 protons. Precision measurements of the cosmic ray antiproton flux are as important as measurements of cosmic ray positrons since both species are antiparticles that have to be created in high-energy processes rather then just being accelerated from the interstellar medium by a passing shock wave.

As discussed in Sect. 3.1, AMS has observed an excess in the positron flux. These data generated many interesting theoretical models including collisions of dark matter particles, astrophysical sources, and collisions of cosmic rays. Some of these models also include specific predictions on the antiproton flux.

As an example, Fig. 5 shows the AMS antiproton spectrum and the antiproton-to-proton flux ratio together with the four recent theoretical predictions for models with dark matter annihilation and cosmic ray collisions [35–37]. As shown the current uncertainties of the modeling need to be further improved before a definitive theoretical interpretation of the origin of cosmic ray antiprotons is possible. This shows the importance of comparing models with all the available AMS data, including also the data on electrons, positrons, protons, and nuclei. The accuracy of theoretical predictions can be improved with the latest AMS results on the fluxes of primary and secondary cosmic rays and their ratios to the models. The continuing AMS measure-

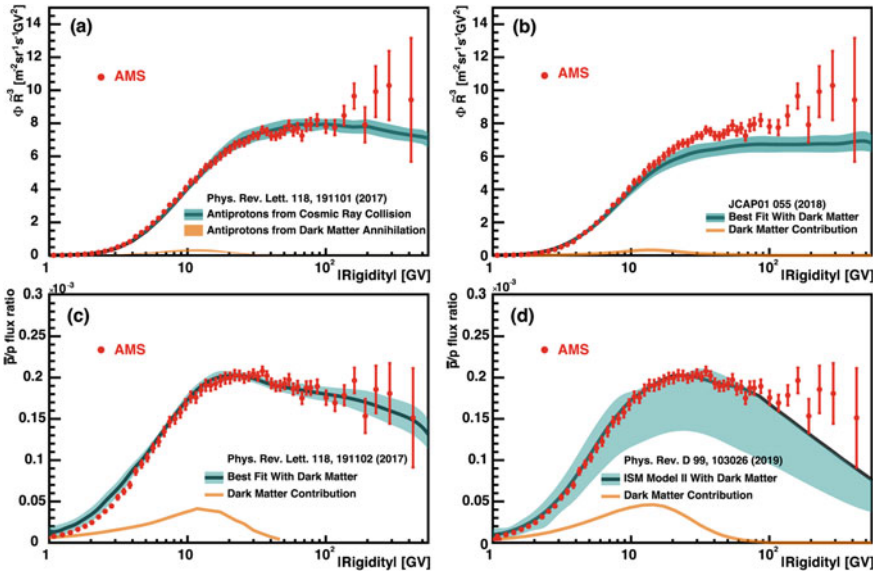

Fig. 5 **a**, **b** The AMS antiproton spectrum and **c**, **d** the antiproton-to-proton flux ratio (red data points) together with four recent theoretical models (black lines), their uncertainties (blue bands), and the contributions from dark matter annihilation (yellow lines) [35–37]

ments of the antiproton spectrum to the highest rigidity with improved accuracy, as well as its detailed time dependent variations, will also provide a crucial input to understanding of the origin of antiprotons in the cosmos.

4 Results on Solar Modulation of CR

In order to reach the Earth's atmosphere, the galactic CR have to pass through the heliosphere, interacting with the solar wind plasma and the solar magnetic field. We have the so-called *Solar modulation* (SM) of CR, that is a time, space, energy, and particle-dependent phenomenon that arises from basic transport processes of CR in the heliosphere [38]. As a result of SM, the measured flux below 30 GeV, is different from the galactic flux, i.e. not affected by the SM. The solar activity has a cycle which period is ∼11 years, during which it increases reaching a maximum and then decreases again. The intensity of cosmic ray radiation is correlated (or rather anticorrelated) with the activity of the sun. Another is the 22-year cycle of the Sun's magnetic field polarity, which reverses every 11 years during the maxima of the solar cycle and that gives a charge-sign dependent effect on CR fluxes.

The study of CR as a function of time and energy allows the study of solar modulation, i.e. of solar activity. Modelling of the heliospheric effects is a complex matter,

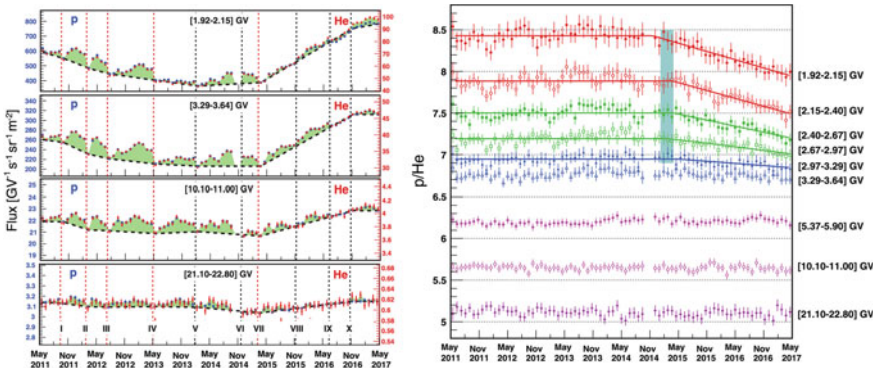

Fig. 6 On the left: The AMS proton (blue, left axis) and helium (red, right axis) fluxes as function of time for 4 rigidity bins. The error bars are the quadratic sum of the statistical and time dependent systematic errors. Detailed structures (green shading and dashed lines to guide the eye) are clearly present below 40 GV. The vertical dashed lines denote boundaries between these structures. On the right: the AMS proton/helium flux ratio as function of time for 9 characteristic rigidity bins. The errors are the quadratic sum of the statistical and time dependent systematic errors

as of today there are very few direct measurements of CR fluxes to correlate with continuous changing solar activities along the extended period of a solar cycle. The large acceptance and high precision of AMS allow us to perform accurate measurements of the fluxes as functions of time and energy with unprecedented precision over at least one complete solar cycle. As of today, AMS as already published the measurements of proton, Helium, electron and positron fluxes as a function of time, with a time granularity corresponding to one Bartels rotation (27 days) and is currently working on the measurements of fluxes in time of the other species of CR. This provides unique information to probe the dynamics of solar modulation, to allow the improvement of constraints for dark matter searches, to investigate the processes of galactic cosmic ray propagation, and to reduce the uncertainties in radiation dose predictions for deep space human exploration.

The time dependence of the proton and helium fluxes are shown in Fig. 6 (left) for 8 characteristic rigidity bins. As seen, both the proton and helium fluxes have fine time structures each with maxima and minima. The structures in the proton flux and the helium flux are nearly identical in both time and relative amplitude. In general, the amplitudes of the structures decrease progressively with rigidity. The precision of AMS enables us to observe these structures up to 40 GV. The amplitudes of the structures are reduced during the time period, which started one year after solar maximum (i.e. starting March 2015), when the proton and helium fluxes steadily increase. As shown in Fig. 6 (right), the p/He ration as a function on time is consistent with a constant above 3.29 GV. Below 3.29 GV, the observed /He flux ratio is steadily decreasing with time after the solar maxima. This behaviour it has been observed for the first time and shows a new and important feature regarding the propagation of

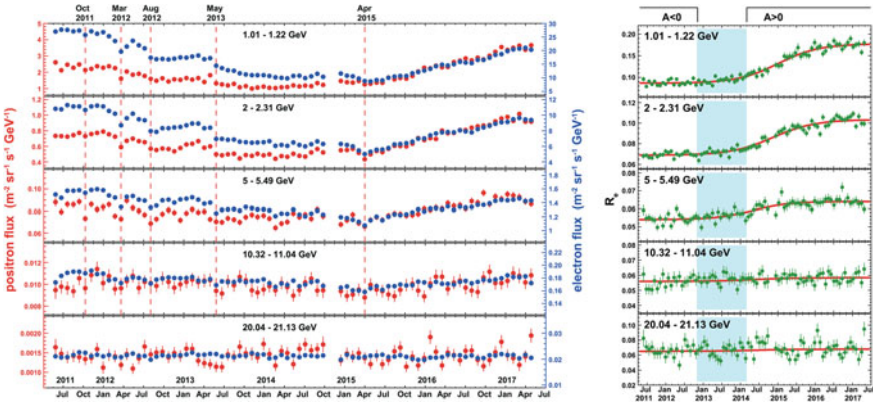

Fig. 7 Left: Fluxes of primary cosmic-ray positrons (red, left axis) and electrons (blue, right axis) as functions of time, for five characteristic bins. The error bars are the statistical uncertainties. Prominent and distinct time structures visible in both the positron spectrum and the electron spectrum and at different energies are marked by dashed vertical lines. Right: The ratio R_e of the positron flux to the electron flux as a function of time. The error bars are statistical. The polarity of the heliospheric magnetic field is denoted by $A < 0$ and $A > 0$. The period without well-defined polarity is marked by the shaded area

lower energy cosmic rays in the heliosphere. The precision of the AMS data provides information for the development of refined solar modulation models [39, 40].

Figure 7 (left) shows the AMS measurements of the time and energy dependence electron and positron fluxes as a function of time for five characteristic energy bins. Both electron and positron fluxes show short-time structures, on the time scale of months. The data show a clear evolution of the fluxes with time at low energies that gradually diminishes towards high energies [**?**]. Both fluxes exhibit profound short- and long-term variations. The short-term variations occur simultaneously in both fluxes with approximately the same relative amplitude. Viceversa, the long-term time structure appear with different relative amplitude for electrons and positrons. This can be clearly seen from Fig. 7 (right) that shows the electron/positron ratio as a function of time in five characteristic energy bins of the fluxes. The short-term variations in the ratio largely cancel, and a clear overall long-term trend appears. At low energies, is flat at first, then smoothly increases after the time of the solar magnetic field reversal, to reach a plateau at a higher amplitude.

Since electrons and positrons differ only in charge sign, their simultaneous measurement offers a unique way to study charge-sign dependent solar modulation effects. For the first time, the charge-sign dependent modulation during solar maximum has been investigated in detail by leptons alone. These data allow comprehensive studies of the energy and charge-sign dependence of short-term effects on the time scale of months, related to solar activity [41, 42], and long-term effects on the time scale of years, related to the 22-year cycle of the solar magnetic field polarity.

5 Conclusions

The AMS experiment has collected more then 190 billion cosmic rays and it will continue to collect data for the lifetime of the International Space Station (2028 and beyond). The current AMS results on CR bring to a puzzled scenario. Electrons and positrons of high energies originate from different sources. In particular, the high energy positrons source, seems to be compatible both with Dark Matter and Pulsars hypothesis. In the future, collecting more statistics, AMS will be able to shed a light on the nature of the source.

The AMS results on CR nuclei, show that primary and secondary nuclei have at least two distinct classes of rigidity dependence but that the rigidity dependence of the two secondary classes is distinctly different from the rigidity dependence of the two primary classes. These are new and unexpected properties of CR. These unexpected results together with ongoing measurements of heavier elements in cosmic rays will enable us to determine how many classes of rigidity dependence exist in both primary and secondary cosmic rays and provide important input to the development of the theoretical models.

For the first time, AMS allows the investigation of charge-sign dependent modulation effect during solar maximum by leptons alone with the measurement of time evolution of electron and positron fluxes. The AMS proton and helium fluxes, show a different behaviour in time below 3.29 GV. This behaviour it has been observed for the first time and shows a new and important feature regarding the propagation of lower energy cosmic rays in the heliosphere. The understanding of solar modulation effects on CR, is fundamental not only to have a correct interpretation of the measured CR fluxes but also to addresses a prerequisite for modeling space weather effects, which is an increasing concern for space missions and air travelers. The study of these effects has been limited for long time by the scarcity of long-term CR data on different species, and by the poor knowledge of the local interstellar spectra. A continuous stream of time-resolved and multichannel CR data is being provided by the AMS.

AMS will continue collecting data through the life of the ISS exploring the physics of complex anti-matter (anti-He, anti-C, etc.), the physics of dark matter (anti-deuterons, anti-protons, and positrons), the physics of cosmic-ray nuclei across the periodic table, and study solar physics over the entire solar cycle.

References

1. P. Blasi et al., Astron. Astrophys. Rev. **21**, 70 (2013)
2. P. Chardonnet et al., Phys. Lett. B **409**, 313–320 (1997)
3. A.G. Mayorov et al., Bull. Russ. Acad. Sci.: Phys. **75**(3), 2011
4. M. Aguilar et al., Phys. Rev. Lett. **114**, 171103 (2015)
5. O. Adriani et al., Phys. Rev. Lett. **111**, 081102 (2013)
6. M. Ackermann et al., Phys. Rev. Lett. **108**, 011103 (2012)
7. C. Grimani et al., Astron. Astrophys. **392**, 287 (2002)

8. M. Boezio et al., Adv. Space Res. **27**, 669 (2001)
9. M. Aguilar et al., Phys. Lett. B **646**, 145 (2007)
10. S.W. Barwick et al., Astrophys. J. **498**, 779 (1998)
11. M.A. DuVernois et al., Astrophys. J. **559**, 296 (2001)
12. M. Aguilar et al., Phys. Rev. Lett. **122**, 041102 (2019)
13. C.H. Chen et al., Cosmol. Astropart. Phys. **03**, 041 (2017)
14. Y. Bai et al., Phys. Rev. D **97**, 115012 (2018)
15. N. Tomassetti et al., Astrophys. J. Lett. **803**, L15 (2015)
16. D. Hooper et al., Phys. Rev. D **96**, 103013 (2017)
17. S. Profumo et al., Phys. Rev. D **97**, 123008 (2018)
18. D. Hooper et al., Cosmol. Astropart. Phys. **01**, 025 (2009)
19. T. Linden et al., Astrophys. J. **772**, 18 (2013)
20. M. Graziani et al., Proc. Sci. **367** (2019)
21. M. Graziani et al., J. Phys. Conf. Ser. **1468**, 1 (2020)
22. M. Aguilar et al., Phys. Rev. Lett. **115**, 211101 (2015)
23. O. Adriani et al., Science **69**, 171103 (2011)
24. A.E. Vladimirov et al., Astrophys. J. **752**, 68 (2012)
25. N. Tomassetti et al., Astrophys. J. **803**, L15 (2015)
26. R. Aloisio et al., Astron. Astrophys. **583**, A95 (2015)
27. N. Tomassetti et al., Phys. Rev. D **92**, 081301(R) (2015)
28. N. Tomassetti, Astrophys. J. **815**, L1(R) (2015)
29. Y. Ohira et al. (2015). arXiv:1506.01196
30. M. Aguilar et al., Phys. Rev. Lett. **126**, 081102 (2021)
31. M.J. Boschini et al., Astrophys. J. **840**, 115 (2017)
32. C. Evoli et al., Phys. Rev. D **99**, 103023 (2019)
33. I.A. Grenier et al., Annu. Rev. Astron. Astrophys. **53**, 199 (2015)
34. G. Jóhannesson et al., Astroph. J. **824**, 16 (2016)
35. A. Cuoco et al., Phys. Rev. Lett. **118**, 191102 (2017)
36. I. Cholis et al., Phys. Rev. D **99**, 103026 (2019)
37. M.Y. Cui et al Phys. Rev. Lett. **118**, 191101 (2017)
38. M.S. Potgieter, Living Rev. Sol. Phys. **10**, 3 (2013)
39. L.F. Burlaga et al., Astrophys. J. **407**, 347 (1993)
40. Jr.G. Newkirk et al., Res. Space Phys. **86**, 5387 (1981)
41. H.V. Cane, Space Sci. Rev. **93**, 55 (2000)
42. M.S. Potgieter et al., Astrophys. J. **403**, 760 (1993)